

Control of Voltage Source Inverter with an LCL Filter without Voltage Sensors

Abstract. The voltage source inverter with LCL filter has to adopt damping method to suppress the resonance of LCL filter, which increases of losses and sensors. With virtual flux estimation idea, grid voltage-sensor-less technology is applied to design observers for the grid voltage, capacitor voltage and current. The observed grid voltage and capacitor voltage is used to realize voltage orientation control and grid current compensation for unit power factor. The observed capacitor current was fed forward to restrain LCL response and keep the control stable. The simulation results verify the correctness of observes design and the control method.

Streszczenie. W artykule analizuje się przekształtnik o źródle napięciowym VSI z filtrem LCL w zastosowaniu do sieci elektrowni wiatrowych. Analizę przeprowadza się na podstawie monitorowania napięcia sieci, prądu sieci i napięcia na kondensatorze. (Sterowanie przekształtnikiem napięciowym z filtrem LCL bez konieczności używania czujników napięcia)

Keywords: voltage source inverter (VSI); LCL filter; grid voltage-sensor-less control; virtual flux observing

Słowa kluczowe: przekształtnik napięciowy VSI, filtr LCL.

1. Introduction

In the wind power system, voltage source inverter (VSI) with an LCL filter (LCL-VSI) is used for better filtering of the grid current [1]-[3]. The resonance of LCL filter often makes the control system unstable. As a solution of this problem, passive damping (PD) or active damping (AD) methods are generally adopted [4]-[6]. However, PD method brings extra power loss and AD method increases additional sensors. For these reasons, grid voltage-sensor-less technology is adopted in order to lower the system cost [7]-[11]. The virtual flux estimation idea is studied to design grid voltage observer, capacitor voltage observer and capacitor current observer only used the dc-link voltage and the converter side current [11]. The grid current is compensated for unit power factor used the converter current feedback control indirectly. The capacitor current from the observer is forward fed back to restrain LCL response problem and keep the control stable. The simulation is performed using Matlab and the simulation results verify the correctness of observer designed and the control method.

2. The mathematical model of the LCL-VSI

Fig. 1 shows the structure of LCL-VSI. Assuming the positive direction of the grid currents is from grid side to converter side, by the circuit theory, the mathematical equation of LCL-VSI in static $\alpha\beta$ coordinate is as following:

$$(1) \quad \begin{cases} u_i(\alpha, \beta) = -R_i i_{i(\alpha, \beta)} - L_i \frac{di_{i(\alpha, \beta)}}{dt} + u_c(\alpha, \beta) \\ u_c(\alpha, \beta) = -R_g i_{g(\alpha, \beta)} - L_g \frac{di_{g(\alpha, \beta)}}{dt} + u_g(\alpha, \beta) \\ i_{i(\alpha, \beta)} = i_g(\alpha, \beta) - i_{cf}(\alpha, \beta)(t) = i_g(\alpha, \beta) - C_f \frac{du_{c(\alpha, \beta)}}{dt} \\ C_d \frac{du_{dc}}{dt} = i_\alpha(t)s_\alpha + i_\beta s_\beta - \frac{u_{dc}}{R_L} \end{cases}$$

The mathematical control equation of LCL-VSI in the rotating $d-q$ coordinate is as following:

$$(2) \quad \begin{cases} u_{i(d, q)} = u_{c(d, q)} - (R_i + sL_i)i_{i(d, q)} \pm \omega L_i i_{i(d, q)} \\ u_{c(d, q)} = u_{g(d, q)} - (R_g + sL_g)i_{g(d, q)} \pm \omega L_g i_{g(d, q)} \\ C_d \frac{du_{dc}}{dt} = 1.5(i_{id}s_d + i_{iq}s_q) - u_{dc}/R_L \end{cases}$$

where, $u_{i(\alpha, \beta)}$, $i_{i(\alpha, \beta)}$ and $u_{i(d, q)}$, $i_{i(d, q)}$ are the converter side voltages and currents in $\alpha\beta$ coordinate and in $d-q$ coordinate; $u_{c(\alpha, \beta)}$, $i_{cf(\alpha, \beta)}$ and $u_{c(d, q)}$, $i_{cf(d, q)}$ are the capacitor side voltages and currents in $\alpha\beta$ coordinate

and in $d-q$ coordinate; $u_{g(\alpha, \beta)}$, $i_{g(\alpha, \beta)}$ and $u_{g(d, q)}$, $i_{g(d, q)}$ are the grid side voltages and currents in $\alpha\beta$ coordinate and in $d-q$ coordinate; C_d is the dc-link filter capacitor; u_{dc} is the dc-link voltage; R_L is the dc-link load; s_α , s_β and s_d , s_q is the switch function in $\alpha\beta$ coordinate and in $d-q$ coordinate.

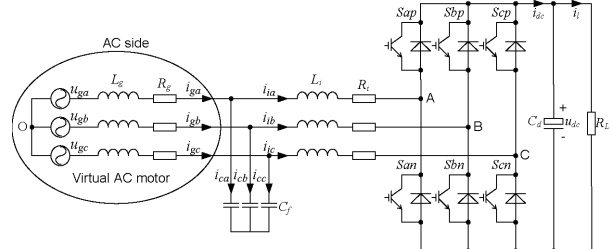


Fig.1. Structure diagram of LCL-VSI

3. Stable analysis of LCL-VSI

Fig. 2 shows the diagram of the current control loop with the converter current as the feedback.

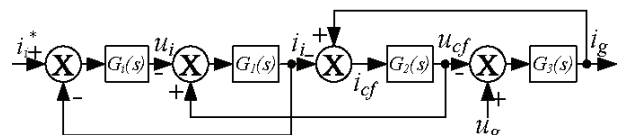


Fig.2. Diagram of current loop

$$\text{where, } G_1(s) = \frac{1}{L_i s}, \quad G_2(s) = \frac{1}{C_f s}, \quad G_3(s) = \frac{1}{L_g s}, \\ G_i(s) = k_{ip} \frac{s + \tau_i}{s}.$$

By the Fig. 2, the open-loop transfer function is obtained:

$$(3) \quad G_o(s) = \frac{k_{ip}(s + \tau_i)}{s} \cdot \frac{s^2 L_g C_f + 1}{s^3 L_i L_g C_f + s(L_g + L_i)}$$

The coefficient of s^2 in the denominator is zero, which means that the control system must be unstable, according to Routh-Hurwitz stable theory. As a result the passive or active damping method should be employed to keep the system stable.

Here, the capacitor current is fed forward into the controller output to suppress the response of the LCL and make the current loop control stable. The method is shown in Fig. 3.

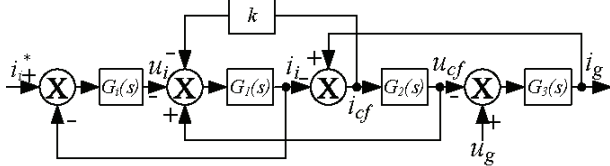


Fig.3. Diagram of current loop with AD

From Fig. 3, the open-loop transfer function is obtained:

$$(4) \quad G_o(s) = \frac{k_ip(s+\tau_i)}{s} \cdot \frac{s^2L_gC_f+1}{s^3L_iL_gC_f+s^2kL_iC_f+s(L_g+L_i)}$$

It is evidence that the coefficient of \$s^2\$ in the denominator is not zero and the control system may be stable by choosing the appropriate \$k\$ value.

4. Grid voltage-sensor-less control method

For the control of the LCL-VSI, the three-phase converter-side currents and the dc-link voltage need to be detected. The grid voltage can be obtained without sensor if the voltage-sensor-less technology is used. The grid voltage and the LCL capacitor voltage and current can be reconstructed with the converter-side current, the dc-link voltage and the switch function.

4.1 The virtual flux observer

According to the virtual flux observer [11], the grid voltage expression under the two-axis static \$\alpha\$-\$\beta\$ coordinate is obtained:

$$(5) \quad \begin{cases} -u_{g\alpha} = \omega\psi_\beta = \omega \int (R_g i_{g\beta} + L_g \frac{di_{g\beta}}{dt} + u_{c\beta}) dt = \omega \int u_{g\beta} dt \\ u_{g\beta} = \omega\psi_\alpha = \omega \int (R_g i_{\alpha} + L_g \frac{di_{\alpha}}{dt} + u_{c\alpha}) dt = \omega \int u_{g\alpha} dt \end{cases}$$

where, \$\psi_\alpha\$ and \$\psi_\beta\$ is the virtual flux of the gird in the two-axis static \$\alpha\$-\$\beta\$ coordinate.

Using the same principle of the relationship between grid virtual flux and grid voltage discussed before, equation of the relationship between grid current and capacitor voltage can be obtained:

$$(6) \quad \begin{cases} \frac{di_{g\alpha}}{dt} = -\omega i_{g\beta}, \frac{di_{g\beta}}{dt} = \omega i_{g\alpha} \\ \frac{du_{c\alpha}}{dt} = -\omega u_{c\beta}, \frac{du_{c\beta}}{dt} = \omega u_{c\alpha} \end{cases}$$

4.2 The capacitor voltage and current observer

The idea of virtual flux with equation (6) is introduced here. Then the capacitor voltage and current observer expression under the two-axis static \$\alpha\$-\$\beta\$ coordinate can be obtained:

$$(7) \quad \begin{cases} u_{c\alpha} = R_i i_{i\alpha} - \omega L_i i_{i\beta} - \omega \int u_{i\beta} dt \\ u_{c\beta} = R_i i_{i\beta} + \omega L_i i_{i\alpha} + \omega \int u_{i\alpha} dt \\ i_{c\alpha} = -\omega C_f u_{c\beta}, i_{c\beta} = \omega C_f u_{c\alpha} \end{cases}$$

In expression (7) the converter output voltage \$u_{i\alpha}\$, \$u_{i\beta}\$ is determined with switch function and dc-link voltage, the expression is:

$$(8) \quad \begin{bmatrix} u_{i\alpha} \\ u_{i\beta} \end{bmatrix} = \sqrt{\frac{2}{3}} \cdot \begin{bmatrix} 1 & -\frac{1}{2} & -\frac{1}{2} \\ 0 & \frac{\sqrt{3}}{2} & -\frac{\sqrt{3}}{2} \end{bmatrix} \cdot \begin{bmatrix} s_a \\ s_b \\ s_c \end{bmatrix} \cdot u_{dc}$$

As the pure integrator will cause a dc component in the result and thus bring errors in control. Two 1st order lower

pass filters are introduced here to replace the pure integrator. The cut off frequency of the filter is \$\omega_c\$, which is equal to grid angle frequency. The transfer function is:

$$(9) \quad u_s(s) = \frac{\sqrt{2}\omega_c}{s + \omega_c} \cdot \frac{\sqrt{2}\omega_c}{s + \omega_c}$$

At the cut off frequency \$\omega = \omega_c\$, the gain of the LP filter is 1 and the phase shift is \$-\pi/2\$, which just equal to the value required. The structure of the observer designed is shown in Fig. 4:

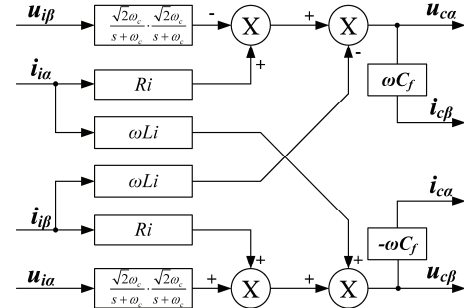


Fig.4. Diagram of capacitor voltage and current observer

4.3 The grid voltage observer

The grid voltage is detected to determine the space vector angle, which is used in coordinate transformation. Since the capacitor voltage can be detected by the voltage observer, according to equation (1), the expression of the grid observer is:

$$(10) \quad \begin{cases} u_{g\alpha} = (1 - \omega^2 C_f L_g) u_{ca} + R_g i_{i\alpha} - \omega L_g i_{i\beta} - \omega C_f R_g u_{c\beta} \\ u_{g\beta} = (1 - \omega^2 C_f L_g) u_{c\beta} + R_g i_{i\beta} + \omega L_g i_{i\alpha} + \omega C_f R_g u_{ca} \end{cases}$$

The grid voltage angle and the sine, cosine value used in coordinate transforming is as following:

$$(11) \quad \begin{cases} \theta_s = \tan^{-1}(\frac{u_{g\beta}}{u_{g\alpha}}), u_m = \sqrt{u_{g\alpha}^2 + u_{g\beta}^2} \\ \cos \theta_s = \frac{u_{g\alpha}}{\sqrt{u_{g\alpha}^2 + u_{g\beta}^2}}, \sin \theta_s = \frac{u_{g\beta}}{\sqrt{u_{g\alpha}^2 + u_{g\beta}^2}} \end{cases}$$

With the help of equation (11) the LCL-VSI signal can be transformed to two-axis \$d\$-\$q\$ rotating coordinate frame, which decouples the control signals to \$d\$ and \$q\$ axis. The structure diagram of the grid voltage observer is showed in Fig. 5:

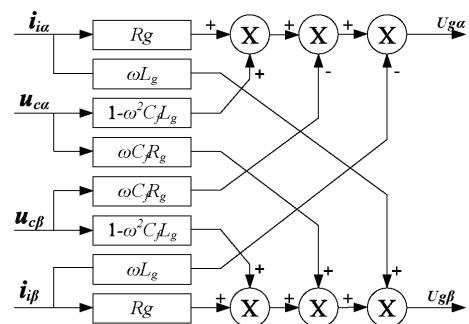


Fig.5. Diagram of grid voltage observer

4.4 System control block

In order to compensate the grid side current, the converter current feedback control is adopted, in which the grid current is constructed by capacitor voltage and converter current by the following equation:

$$(12) \quad \begin{cases} i_{g\alpha} = C_f \frac{du_{c\alpha}}{dt} + i_{i\alpha} = -\omega C_f u_{c\beta} + i_{i\alpha} \\ i_{g\beta} = C_f \frac{du_{c\beta}}{dt} + i_{i\beta} = \omega C_f u_{c\alpha} + i_{i\beta} \end{cases}$$

Converting equation (7) to two-axis rotating $d-q$ coordinate frame gives:

$$(13) \quad \begin{cases} (1-\omega^2 C_f L_g) u_{cd} = u_{gd} - R_g i_{id} + \omega L_g i_{iq} + \omega C_f R_g u_{cq} \\ (1-\omega^2 C_f L_g) u_{cq} = u_{gq} - R_g i_{iq} - \omega L_g i_{id} - \omega C_f R_g u_{cd} \end{cases}$$

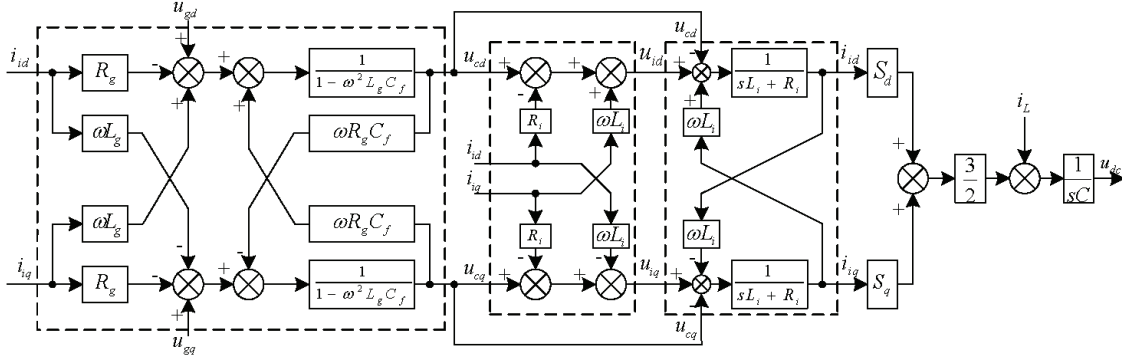


Fig.6. Control diagram of LCL-VSI using converter current feedback

5. Simulation and result analysis

In order to test the voltage-sensor-less control, The simulation is carried out in Matlab. The electrical and control parameters are shown in Table1, where f is grid frequency and f_{sw} is switching frequency. The simulation result is showed in Fig. 7 ~12.

Tab. 1 Electrical and control parameters in simulation

Parameter	Value
e_a/V	380
f/Hz	50
U_{dc}/V	600
$C_d/\mu F$	18800
$L_g/\mu H$	80
$C_f/\mu F$	170
$L_i/\mu H$	468
R_d/Ω	0.1
R_L/Ω	4.8
f_{sw}/Hz	3000
k	4.3

Fig. 7 shows the real signal and observed signal about the grid voltage U_{ga} and U_{gb} in stable state. Fig. 8 shows the real signal and observed signal about the voltage of LCL capacitor U_{ca} and U_{cb} in stable state. It can be seen that there are no phase shift between the real and observed signals, which means that the observer is correct.

Fig. 9 shows the PLL output, designed with the output of the observer, and the real angle waveform. It can be seen that there is no phase shift and its linearity is good enough. (For convience here, the real angle waveform is subtracted with a constant 2).

Fig. 10 shows the phase A-phase gird voltage and grid current when working in unit power factor. The phase error between the two signals is entirely same, which means that the grid current is indirectly controlled with the control of converter-side current.

Fig. 11 shows the three-phase grid current in stable state. From the waveform it can be seen that the voltage-sensor-less technology works well. Fig. 12 shows the

Converting equation (12) to two-axis rotating dq coordinate frame gives:

$$(14) \quad \begin{cases} i_{gd} = i_{id} + i_{cd} = i_{id} - \omega C_f u_{cq} \\ i_{gq} = i_{iq} + i_{cq} = i_{iq} + \omega C_f u_{cd} \end{cases}$$

Then, the diagram of the converter current feedback control of the LCL-VSI is shown in Fig. 6:

dynamic waveform of the grid current under the same condition. It can be seen that, the system recovered to stable state within only 2-3 periods, which means that the system has a good dynamic response.

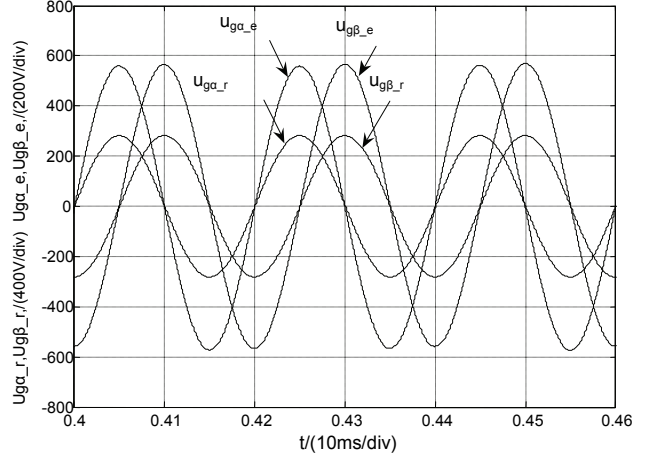


Fig.7. Real and estimated waveforms of gird voltage

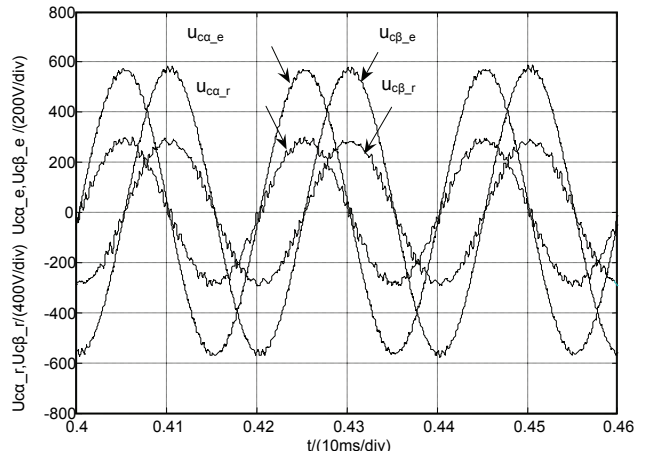


Fig.8. Real and estimated waveforms of cap voltage

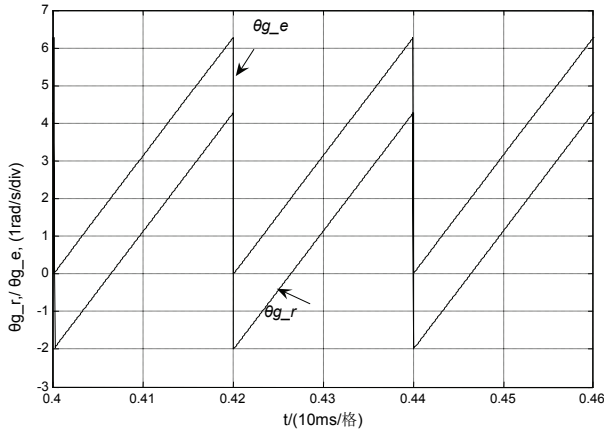


Fig.9. Real and estimated waveforms of grid voltage angle

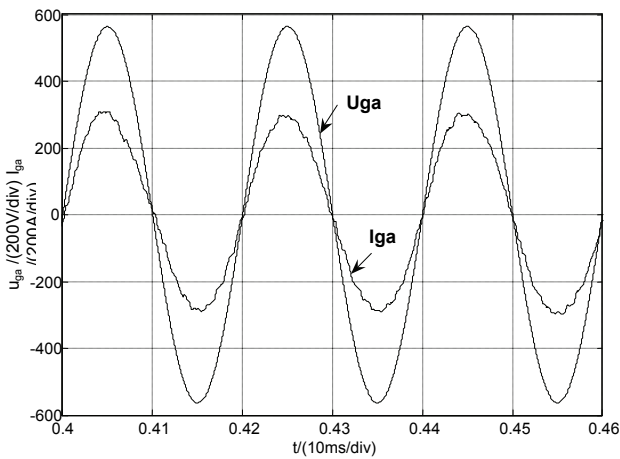


Fig.10. A-phase grid voltage and current waveforms in PF=1

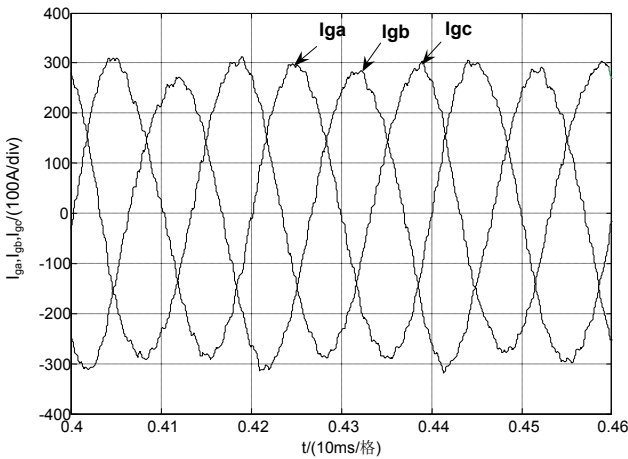


Fig.11. Waveforms of three-phase grid current in steady-state

5. Conclusion

By introducing virtual flux estimation ideas and voltage-sensor-less technology into the LCL-VSI, which detects the LCL capacitor voltage and grid voltage by state observers, the related sensor can be removed in the LCL resonance control scheme. In addition, because the LP filter is used to replace the pure integrator, the system has better capability of load rejection. As the simulation has shown, by adopting the grid voltage-sensor-less technology to control LCL-VSI, the number of sensor is reduced, which reduces the cost of the system.

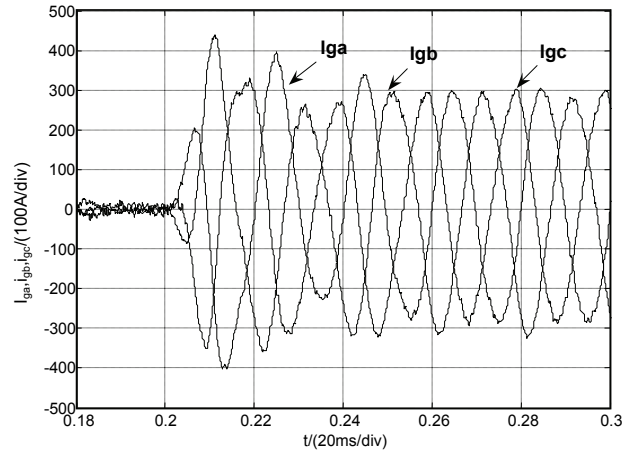


Fig.12 Waveforms of grid currents during output power steps

REFERENCES

- [1] F. Blaabjerg, R. Teodorescu, M. Liserre, A. V. Timbus, Overview of control and grid synchronization for distributed power generation systems, *IEEE Transactions on Industry Applications*, 53(2006), No.5, 1398- 1409
- [2] B. Singh, B. N. Singh, A. Chandra, et al., A review of three-phase improved power quality AC-DC converters, *IEEE Trans. On Industrial Electronics*, 51(2004), No.3, 641- 660
- [3] Dannehl J., Wessels C., Wilhelm F. F., Limitations of Voltage-Oriented PI Current Control of Grid-Connected PWM Rectifiers With LCL Filters, *IEEE Trans. On Industrial Electronics*, 56(2009), No.2, 380- 388
- [4] M. Liserre, F. Blaabjerg, S. Hansen, Design and control of an LCL-filter-based three-phase active rectifier, *IEEE Trans. On Industry Applications*, 41(2005), No.5, 1281-1291
- [5] M. Prodanovic and T. C. Green, Control and filter design of three-phase inverters for high power quality grid connection, *IEEE Trans. On Power Electronics*, 18(2003), No.1, 373-380
- [6] Twining E., Donald G. H., Grid current regulation of a three-phase voltage source inverter with an LCL input filter, *IEEE Trans. on Industry Applications*, 18(2003), No.3 , 888-895
- [7] Malinowski M., Kamierkowski M., Hansen S. Blaabjerg F. et al., Virtual-Flux-Based Direct Power Control of Three-Phase PWM Rectifiers, *IEEE Trans. On Industry Applications*, 37(2001), No.4, 1019-1027
- [8] Malinowski M. and Bernet S., A Simple Voltage Sensorless Active Damping Scheme for Three-Phase PWM Converters With an LCL Filter, *IEEE Trans. On Industrial Electronics*, 55(2008), No.4, 1876-1880
- [9] Agriman I., Blasko V., A Novel Control Method of a VSC Without AC Line Voltage Sensors, *IEEE Trans. Industry Applications*, 39(2003), No.2, 519- 524
- [10] Ohnuki T., Miyashita O., Lataire Ph., Control of a Three-Phase PWM Rectifier Using Estimated AC-Side and DC-Side Voltages, *IEEE Trans. On Power Electronics*, 14(1999), No.2, 222- 226
- [11] Suul J. A., Luna A., Rodriguez P., et al., Voltage-Sensor-Less Synchronization to Unbalanced Grids by Frequency-Adaptive Virtual Flux Estimation, *IEEE Trans. On Industrial Electronics*, 59(2011), No.7, 2910- 2923

Authors: Han WANG, Department of Electrical Engineering, Shanghai Jiao Tong University, No. 800 of Dongchuan Road, Minhang District, Shanghai, CHINA, winseaner@163.com